# SORPTION AND SURFACE ENERGY PROPERTIES OF THERMALLY MODIFIED SPRUCE WOOD COMPONENTS

## Susanna Källbom*†

PhD Student
Division of Building Materials
KTH Royal Institute of Technology
Stockholm SE-100 44, Sweden
E-mail: susanna.kallbom@byv.kth.se

## Michael Altgen

Postdoctoral Researcher
Wood Biology and Wood Products
Georg-August University Göttingen
Göttingen DE-37077, Germany
and
Department of Bioproducts and Biosystems
Aalto University
P.O. Box 16300, Aalto FI-00076, Finland
E-mail: michael.altgen@aalto.fi

## Holger Militz

Professor
Wood Biology and Wood Products
Georg-August University Göttingen
DE-37077 Göttingen, Germany
E-mail: hmilitz@gwdg.de

## Magnus Wålinder†

Professor
Division of Building Materials
KTH Royal Institute of Technology
SE-100 44 Stockholm, Sweden
E-mail: magnus.walinder@byv.kth.se

(Received April 2018)

**Abstract.** The objective of this work is to study the water vapor sorption and surface energy properties of thermally modified wood (TMW) components, ie wood processing residuals in the form of sawdust. The thermal modification was performed on spruce wood components using a steam-pressurized laboratory-scale reactor at two different temperature ($T$) and relative humidity (RH) conditions, $T = 150°C$ and RH = 100% (TMW150), and $T = 180°C$ and RH = 46% (TMW180). A dynamic vapor sorption (DVS) technique was used to determine water vapor sorption isotherms of the samples for three adsorption-desorption cycles at varying RH between 0% and 95%. Inverse gas chromatography (IGC) was used to study the surface energy properties of the samples, including dispersive and polar characteristics. The DVS results showed that the EMC was reduced by 30-50% for the TMW samples compared with control samples of unmodified wood (UW) components. A lower reduction was, however, observed for the second and third adsorption cycles compared with that of the first cycle. Ratios between EMC of TMW and that of UW samples were lower for the TMW180 compared with the TMW150 samples, and an overall decrease in such EMC ratios was observed at higher RH for both TMW samples. The IGC results showed that the dispersive contribution

to the surface energy was higher at lower surface coverages, ie representing the higher energy sites, for the TMW compared with the UW samples. In addition, an analysis of the acid-base properties indicated a higher $K_B$ than $K_A$ number, ie a higher basic than acidic contribution to the surface energy, for all the samples. A higher $K_B$ number was also observed for the TMW compared with the UW samples, suggested to relate to the presence of ether bonds from increased lignin and/or extractives content at the surface. The $K_B$ was lower for TMW180 compared with TMW150, as a result of higher modification temperature of the first, leading to cleavage of these ether bonds.

## INTRODUCTION

Thermal modification of solid wood and the resulting durability and dimensional stability enhancements have been widely studied and documented during the last decades (Hill 2006; Esteves and Pereira 2009). Few studies have, however, focused on thermal modification of wood components, eg wood processing residuals such as sawdust, grindings, or shavings. An idea and main motive of this study is that such thermally modified wood (TMW) components could be interesting for use in wood plastic composites (WPC); ie a value adding concept of wood residuals, and with a potential to significantly enhance also the in-service properties of WPC such as increased moisture resistance, dimensional stability, and resistance against attack by microorganisms. Studies of thermal modification of wood components for the use in particleboards have been conducted by Paul et al (2006) and Medved et al (2012); analyzing the effects on dimensional stability, and also strength properties (Andrade et al 2016). They reported lowered hygroscopicity and increased dimensional stability as a result of the thermal modification. Other studies by Weigl et al (2013) indicated lowered water retention, reduced sorption isotherms (Hoffmeyer et al 2003), and minor variations in surface properties (Liu et al 1998) of TWM, compared with unmodified wood (UW) components and fibers. However, limited research has been carried out on their water vapor sorption properties, and none with additional links to their surface energy properties.

Earlier studies of the water vapor sorption behavior of TMW have shown significant reduction in hygroscopicity compared with UW controls,

eg for Scots pine (Engelund et al 2010; Hill et al 2012), Sitka spruce (Hill et al 2010; Endo et al 2016) and Norway spruce (Pfriem et al 2010; Källbom et al 2016; Majka et al 2016). The preferential thermal degradation of hemicelluloses, which contain the highest concentration of water-accessible hydroxyl groups among the cell wall polymers (Runkel 1954; Runkel and Lüthgens 1956), reduces the number of water sorption sites in wood. Furthermore, cross-linking reactions within the cell wall matrix limit the access to the remaining sorption sites (Tjeerdsma et al 1998). However, recent studies (Hill et al 2012; Majka et al 2016) evidenced the occurrence of a reversible reduction in hygroscopicity in addition to any irreversible changes. This conclusion was based on the analysis of several adsorption-desorption cycles for TMW using a so-called dynamic vapor sorption (DVS) technique or different relative humidity (RH) conditions controlled by salt solution, showing a decrease of sorption hysteresis comparing the first with the second sorption cycle. Annealing and ultra-structural realignments of amorphous polymers by high-temperature drying above their softening point have been suggested as a potential cause. Thereby, the amorphous cell wall matrix retains a certain amount of internal stresses after modification, which can be relaxed by exposure to high RH or water-soaking at room temperature (Altgen and Militz 2016; Endo et al 2016).

Analysis of the surface characteristics of wood components, such as surface energy and acid-base properties, can provide important information needed for the design of composite materials, and understanding of the interaction between

glues, coatings, and also other wood components. These properties have often been studied using contact angle measurements, suitable for analysis of solid wood products. For the examination of wood components, such as particles or fibers, an advantageous approach is to use inverse gas chromatography (IGC). This technique is based on interactions between the component material, with unknown properties, and various nonpolar and polar vapor probes with known properties. The surface energy properties are related to the surface chemical composition, eg functional groups or extractives present at the surface (Tshabalala 1997). Several studies have applied the IGC technique to study the surface energy properties of milled wood components, ie wood flour (Kamdem et al 1993; Tshabalala 1997; Liu et al 1998; Wålinder and Gardner 2000, 2002; Peterlin et al 2010; Cordeiro et al 2012). The results from these studies provide single values of the surface energy, representing the highest energy sites of the surface based on very low solute concentration. A recently developed approach (Thielmann et al 2007) enables IGC measurements from higher to lower energy sites, characterizing the surface energy heterogeneity. This approach has been used in recent studies for analysis of the dispersive part of the surface energy; showing increased values for TMW components compared with UW (Källbom et al 2015), increased values for increased refiner pressure (from 4 to 8 bar) on wood fibers (Ormondroyd et al 2017), effects on extraction of TMW strips (Källbom et al 2018), and analysis of various natural fibers (Legras et al 2017). Analysis of the acid-base properties of wood components have been performed in earlier IGC studies (de Meijer et al 2000; Wålinder and Gardner 2002; Cordeiro et al 2012), showing a dominant basicity.

Thermal modification of wood has often been performed at atmospheric pressure together with superheated steam where volatile degradation products are allowed to evaporate, and severe drying takes place (Militz and Altgen 2014). The modification process can also take place in a closed reactor system, which accelerates thermal degradation and enables the regulation of the water vapor pressure and the RH during the modification process (Willems et al 2015; Altgen et al 2016c). Altgen et al (2016c) showed for European beech (*Fagus sylvatica* L.) wood that the mass loss (ML) obtained in a closed reactor system is a function of the maximum vapor pressure, and less dependent on the peak temperature ($\leq 180°C$) applied. This was explained by elevated wood MC and the accumulation of carboxylic acids (ie acetic acid) within the wood that catalyzed the thermal degradation of wood at low temperature and high vapor pressure regimes.

By contrast to thermal modification of solid wood, the focus of this work is to study the possibilities for thermal modification of wood components such as processing residuals. The specific objective of this work is to study the water vapor sorption and surface energy heterogeneity and acid-base properties of TMW from spruce, in this case in the form of sawdust, using a steam-pressurized reactor normally used for thermal modification of solid wood. These properties can give valuable information and increased understanding of the interaction between wood components and eg polymers in a composite material.

## MATERIALS AND METHODS

### Materials

Norway spruce (*Picea abies* Karst.) sawdust, originating from a circular saw process, and hereafter called wood components, were collected at Karl Hedin AB sawmill in Krylbo in central Sweden. The wood components were dried for 2 da in a convection oven with a temperature of 40°C, reducing the initial moisture content (MC) from about 54% to about 10%. The wood components were then sifted into different fractions and the size fraction between 18 and 10 mesh (>1.0 and <2.0 mm), giving about 70 g, subsequently used in this study.

### Thermal Modification

Thermal modification of the UW components was performed using a steam-pressurized laboratory-scale treatment reactor (Willems 2009), where

the temperature, pressure, and RH could be regulated. The reactor consisted of a 65-l stainless steel vessel, connected to a water reservoir and a gas washer, controlled by exhaust valves. The thermal modification process included five different steps; 1) application of a prevacuum (ca. 14 kPa); 2) holding step at 50°C for 50 min; 3) temperature increase (12°C/h) to the peak temperature; 4) holding step at peak temperature for 120 min at 0.47 MPa; 5) temperature decrease (−20°C/h) until reaching a pressure of 0.1 MPa. The RH was kept constant throughout the modification process by regulating the pressure in the reactor via an increase in temperature in the water reservoir or by a release of pressure using the exhaust valves. Two different thermal modification processes were executed using two different peak temperature ($T$) and RH conditions, while applying the same constant maximum pressure of 0.47 MPa; resulting in two different TMW component samples: 1) TMW150 ($T = 150°C$, RH = 100%) and 2) TMW180 (T = 180°C, RH = 46%). About 10 g was prepared for each modification. The regulated RH is described in Eq 1.

$$\text{RH} = \frac{P_{\text{vap}}}{P_{\text{sat}}(T)} \cdot 100\%, \qquad (1)$$

where $P_{\text{vap}}$ is the water vapor pressure and $P_{\text{sat}}(T)$ is the temperature-dependent saturated water vapor pressure. The MC was determined before and after the thermal treatment, see Table 2. The extractives content of the wood samples (Table 2) was determined with hot-water extraction, where duplicates of about 3 g of dried wood components (dried overnight at 103°C) were extracted with 200 mL distilled water for 6 h using a Soxhlet apparatus. The amount of water-extractable compounds was determined by measuring the difference in dry weight before and after extraction. In addition, the pH of the water solutions were measured after hot-water extraction (Table 2).

## DVS

Water vapor sorption isotherms of the UW, TMW150, and TMW180 samples, about 20 mg each, were determined using a DVS apparatus (DVS advantage; Surface Measurement Systems Ltd., London, UK). Sorption isotherm measurements, ie determination of the EMC vs the RH for adsorption and desorption, started at 0% RH followed by the holding steps: 5%, 20%, 35%, 50%, 65%, 80%, and 95% RH. The RH was kept constant until a change in sample weight <0.002%/min over a 10 min period, which induced a progression to the next RH level. Thereafter, the corresponding desorption measurements were performed reversing back to 0% RH with the same holding steps. The same procedure was performed in three cycles and the temperature was kept constant at 25°C. The EMC ratio was calculated by relating the EMC of the TMW samples to the EMC of the UW sample at each RH step. A more detailed description of the DVS methodology has been previously published (Hill et al 2012).

## IGC

***Theory.*** The surface energy ($\gamma_{\text{s}}$) of a solid (s) material can be divided into a physical part ($\gamma_{\text{s}}^{d}$), also called the nonpolar or dispersive part, and a chemical part ($\gamma_{\text{s}}^{\text{AB}}$), also called the polar or specific part (see Eq 2). Determination of the dispersive part of the surface energy can be performed by injecting various nonpolar n-alkanes whereas the polar part can be determined indirectly from the specific energy of various polar probes.

$$\gamma_{\text{s}} = \gamma_{\text{s}}^{d} + \gamma_{\text{s}}^{\text{AB}}, \qquad (2)$$

The surface property calculations are based on the net retention volume ($V_{\text{N}}$) of injected gas probes, which is dependent on the time of interaction between these gas probes and the solid surface. As the $V_{\text{N}}$ is corrected for the dead volume (which is the dead time of a noninteracting probe traveling through the sample column), it can be described by Eq 3:

$$V_{\text{N}} = \frac{j}{m} \cdot F \cdot (t_{\text{r}} - t_0) \cdot \frac{T}{273.15}, \qquad (3)$$

where $j$ is a correction factor related to pressure drop, $m$ is the mass of the solid sample, $F$ is the carrier gas flow rate, $t_{\text{r}}$ and $t_0$ are the retention

time and retention time of dead volume measurement, and $T$ is the operating temperature. The new generation IGC approach is based on finite dilution conditions, allowing the determination of a heterogenous character of the surface by sorption measurements at different surface coverages ($n/n_m$). This is regulated by the partial vapor pressure to finite concentration dilution, where the gas probes are injected at various concentrations. Two common approaches for determination of the surface energy using IGC are the Schultz method (Schultz et al 1987) and the Dorris-Gray method (Dorris and Gray 1980). The Schultz method enables for determination of the dispersive and polar part of the surface energy, using the free energy of adsorption $\Delta G_a$ (Fowkes and Mostafa 1978; van Oss et al 1988):

$$\Delta G_a = \Delta G_a^d + \Delta G_a^{AB}, \qquad (4)$$

where $\Delta G_a^d$ and $\Delta G_a^{AB}$ describe the free energy of adsorption for the dispersive and polar parts, respectively. For analysis of the dispersive part of the surface energy, $\Delta G_a^d$ is further described in Eq 5 as:

$$\Delta G_a = \Delta G_a^d = R \cdot T \cdot \ln(V_N) + C, \qquad (5)$$

where $R$ is the universal gas constant, and $C$ is a constant related to the reference state. The $\Delta G_a$ can be combined with the work of adhesion ($W_a$) for nonpolar alkane probes, giving the following correlation (Dorris and Gray 1980):

$$-\Delta G_a = N \cdot a \cdot W_a, \qquad (6)$$

where $a$ is the cross-sectional area of the probe and $N$ is the Avogadro number. $W_a$ is described by Eq 7, including a mean of the dispersive surface tension of the alkane probe in liquid ($l$) form and the dispersive component of the surface energy of the solid.

$$W_a = W_a^d = 2\sqrt{\gamma_s^d \cdot \gamma_l^d}, \qquad (7)$$

where $\gamma_l^d$ is the dispersive part of the surface tension for the alkane probe in liquid form. The dispersive part of the surface energy with the Schultz method approach can then be obtained

according to Eq 8, from plotting $R \cdot T \cdot \ln(V_N)$ as a function of $a\sqrt{\gamma_l^d}$, giving a linear correlation of the alkanes, see Figure 1.

$$\gamma_s^d = \frac{1}{4 \cdot \gamma_l^d} \left( \frac{R \cdot T \cdot \ln(V_N)}{N \cdot a} \right)^2, \qquad (8)$$

For determination of the polar part of the surface energy, the specific free energy of adsorption for the various polar probes is measured. These are found above the linear line of the alkanes (see Fig 1) using the Schultz approach and can be expressed according to Eq 9 as:

$$-\Delta G_a^{AB} = -\left(\Delta G_a - \Delta G_a^d\right) = R \cdot T \cdot \ln\left(\frac{V_N}{V_{N,ref}}\right), \qquad (9)$$

where $V_N$ is the retention volume of a polar probe and $V_{N,ref}$ the retention volume of a hypothetical nonpolar probe with the same $\sqrt{\gamma_l^d}$ as that of the polar probe. The acceptor-donor properties can be determined from the acid-base properties including the $K_A$ and $K_B$ numbers according to the Gutmann method (Gutmann 1978) and based on the approach of Saint Flour and Papirer (1982) using $-\Delta G_a^{AB}$ (valid for a certain temperature) instead of $\Delta H_a^{AB}$. This can be obtained by measuring the specific free energy of adsorption
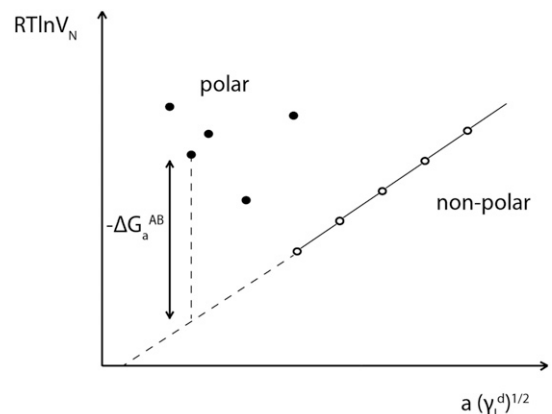


Figure 1. Schematic illustration of the Schultz method showing the retention volume vs the molecular descriptor for determination of the dispersive and the polar part of the surface energy using a series of nonpolar and polar probes.

for the different polar probes, obtained from the retention volume as can be seen in Eq 10.

$$-\Delta G_a^{AB} = DN \cdot K_A + AN^* \cdot K_B, \quad (10)$$

where DN is the donor number of the polar probes and $AN^*$ is the acceptor number.

For determination of the dispersive part of the surface energy using the Dorris-Gray method, see Källbom et al (2015).

## IGC Measurements

IGC was used to determine the physicochemical properties of the wood components, in terms of surface area, surface energy heterogeneity, and acid-base properties. The equipment used was a surface energy analyzer (SEA) from Surface Measurements Systems (SMS Ltd., Alperton, London, UK). The components were initially dried in a ventilated conventional oven for 1 h at 103°C and then packed into silanized glass columns (length 300 mm and inner diameter 4 mm) and fixated at both ends with silanized glass wool. The sample mass was about 200 mg and the packing density about 0.13–0.14 g/cm³ for all the samples. The sample columns were preconditioned in the IGC apparatus for 2 h at 30°C and 0% RH to remove volatiles. Purified helium was used as the carrier gas (flow rate 10 mL/min) and methane was used to determine the dead volume. In the first part of the analysis, the BET (Brunauer Emmet Teller) specific surface area was determined, which was further required as input data for the surface energy analysis. The theory behind the BET specific surface area is described in Källbom et al (2015). The BET specific surface area was determined from octane sorption isotherms in the partial pressure range 5-35% using three sample column replicates. The solvent probes used for analysis of the surface energetics included various n-alkanes; octane, nonane, decane, and undecane for the dispersive part and acetone, acetonitrile, dichloromethane, and ethyl acetate for the polar part. Properties of the various solvent probes can be found in Table 1. The nonpolar probes were supplied by Sigma-Aldrich, and the polar probes by Sigma-Aldrich

and Fluka Analytical. The experiments were conducted at 30°C and 0% RH. In this work, the Dorris-Gray method was used for analysis of the dispersive part, and the Schultz method was used to determine the acid-base properties.

## Thermal Modification

The ML and MC of the two TMW samples (TMW150 and TMW180) can be seen in Table 2. The ML was higher for TMW180 compared with TMW150, indicating that the peak temperature was the most crucial process parameter to determine thermal degradation. This contradicts a previous study on European beech wood modified in the very same treatment reactor, which showed that ML increased as a function of the maximum pressure applied, further indicating a low correlation to the peak temperature (Altgen et al 2016c). In line with Altgen et al (2016c), a higher wood MC was recorded for TMW150 than for TMW180 at the end of the process. Although the presence of water catalyzes thermal wood degradation (Borrega and Kärenlampi 2008), the differences in MC were presumably too small to compensate for the lower peak temperature applied.

However, what sets this study apart from the previous study, besides the different wood species studied, is the sample size and the total amount of wood being treated in the reactor. Altgen et al (2016c) used solid samples (35 × 65 × 800 mm³) with a total of more than 9 kg wood per

Table 1. Properties of the nonpolar and polar inverse gas chromatography probes used.

| Probe | $a$ (Å²)[a] | $\gamma_L^D$ (mJ/m²)[b] | AN*[c] | DN[c] |
|---|---|---|---|---|
| n-octane | 63 | 21.1 | | |
| n-nonane | 69 | 22.4 | | |
| n-decane | 75 | 23.4 | | |
| n-undecane | 81 | 24.2 | | |
| Acetone | 34 | 22.7 | 2.5 | 17.0 |
| Acetonitrile | 21 | 28.7 | 4.7 | 14.1 |
| Dichloromethane | 25 | 39.4 | 3.9 | 0.0 |
| Ethyl acetate | 33 | 23.4 | 1.5 | 17.1 |

[a] The surface area that can be occupied by one probe molecule (Liu et al 1998).
[b] The surface tension of the probe liquids at 25°C (Lide 1995).
[c] AN*, acceptor number; DN, donor number (Gutmann 1978).

Table 2.   Mass loss (ML) and moisture content (MC) of the two thermally modified wood (TMW) component samples (TMW150 and TMW180), and the MC of the unmodified wood (UW) component before thermal modification, together with content of water soluble extractives determined by Soxhlet extraction with hot-water and pH of the water extract.

| Sample | Peak modification temperature (°C) | Maximum pressure (MPa) | ML (%) | MC (%) | Extractives (%) | pH |
|---|---|---|---|---|---|---|
| UW | — | — | — | 4.9 (0.0) | 5.4 | 5.6 |
| TMW150 | 150 | 0.47 | 2.6 (0.4) | 4.3 (0.0) | 4.4 | 4.9 |
| TMW180 | 180 | 0.47 | 4.0 (0.5) | 1.6 (0.2) | 4.8 | 4.7 |

treatment. This lead to a considerable formation of carboxylic acids (ie acetic and formic acid) and other degradation products that accumulated in the wood preferentially under low temperature and high-pressure regimes to facilitate wood degradation. In the current study, only a few grams of wood components were treated in the reactor. The lower amount of wood severely decreased the concentration of carboxylic acid (ie acetic and formic acid) present in the treatment vessel, whereas the smaller size presumably facilitated the vaporization of degradation products because of a higher surface to volume ratio of the components compared with solid wood. This is in line with the results of the Soxhlet extraction (Table 2), that showed a decrease in hot-water extractives compared with the reference and no considerable pH difference between the two treatment conditions. The results indicate that the modes of action involved in thermal degradation of solid wood in a closed reactor system cannot be directly transferred to the thermal modification of the wood components used in this study.

## Sorption Properties

Figure 2 shows the water vapor sorption isotherms for three adsorption-desorption cycles of the UW, TMW150 and TMW180 resulting from the DVS measurements. As can be seen, the sorption isotherms of UW followed the normal type II sorption isotherm and were similar for all the three sorption cycles. As expected, Figure 2 also shows that the thermal treatment significantly reduces the EMC of TMW in comparison with the UW samples. For the first cycle, the EMC was reduced about 30-40% for TMW150 and about 30-50% for TMW180 in relation to UW. Differences between the first and subsequent cycles for both TMW150 and TMW180 could also be observed. In both cases, a noticeable different adsorption curve, ie lower EMC values, were seen for the first cycle compared with the following two cycles. This indicates that a part of the EMC reduction effect resulting from the thermal treatment is reversible because of moisture sorption, in line with Hill et al (2012) and Majka et al (2016). Stronger drying
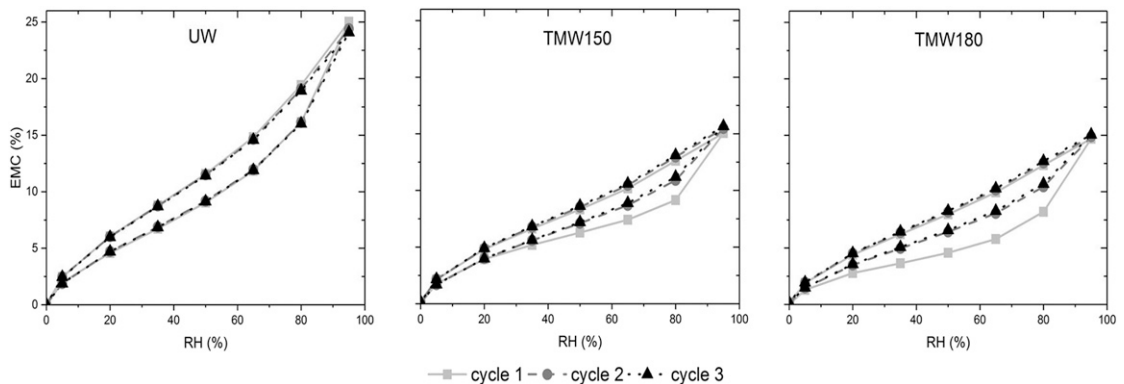


Figure 2.   Water vapor sorption isotherms presented as equilibrium moisture content (EMC) vs relative humidity (RH) for three adsorption-desorption cycles for samples of unmodified wood (UW) components and two different thermally modified wood components and treated at $T = 150°C$ and $RH = 100\%$ (TMW150), and at $T = 180°C$ and $RH = 46\%$ (TMW180), respectively. One three-cycle measurement per sample (∼20 mg) was performed. TMW, thermally modified wood.

during the modification process for the TMW180 than for TMW150, evident from a lower MC recorded after the thermal modification process (Table 2), resulted in a larger reversible part of the EMC reduction. This supports earlier observations that the EMC reduction is not fully irreversible, and that this is related to high-temperature drying during the modification process (Altgen and Militz 2016; Endo et al 2016).

Figure 3 shows the EMC of TMW150 and TMW180 related to that of UW, which is called EMC ratio. An EMC ratio less than one indicates a decrease in EMC by the thermal modification process, and the effectiveness in reducing the EMC by thermal modification increases with decreasing EMC ratio. For the first adsorption cycle, the EMC ratio decreased as a function of RH for low RH values, but increased higher than 80% and 60% RH for TMW150 and TMW180, respectively. The explanation for this behavior may be attributed to the softening of hemicelluloses, which starts above 60% RH (Engelund et al 2013). Softening of amorphous polymers, together with increased swelling could, therefore, cause relaxation of drying stresses retained in the cell wall matrix, thereby removing the drying-related reduction in EMC (Altgen and Militz 2016; Endo et al 2016).

The EMC ratio and sorption isotherms of TMW150 and TMW180 remained virtually unchanged between the second and third sorption cycle. Especially at low RH levels, the EMC reduction was larger for TMW180 than for TMW150, in line with a higher ML for the former. Nevertheless, it is disputable if all drying-stresses are released by water vapor exposure in the DVS, and if the EMC reduction in the second and third cycle is solely based on irreversible chemical changes induced by thermal modification. In a study on the effect of wood drying on hydroxyl accessibility, it was demonstrated recently that full reaccessibility of hydroxyl groups is only achieved by vacuum-impregnation with liquid water (Engelund Thybring et al 2017). Interestingly, however, the EMC ratios of TMW150 and TMW180 further decreased with increasing RH during the second and third cycle of DVS measurements. A similar behavior has been observed for wood that is modified with cross-linking agents (Himmel and Mai 2015). For thermally modified Scots pine sapwood, the decrease in EMC ratio with increasing RH has been assigned to the formation of covalent bonds and cross-links by repolymerisation reactions under dry heat-conditions that hinder the creation of sorption sites by expansion of nanopores (Altgen et al 2016b).

## Surface Properties

The BET specific surface area were similar for the three different samples, but with a somewhat
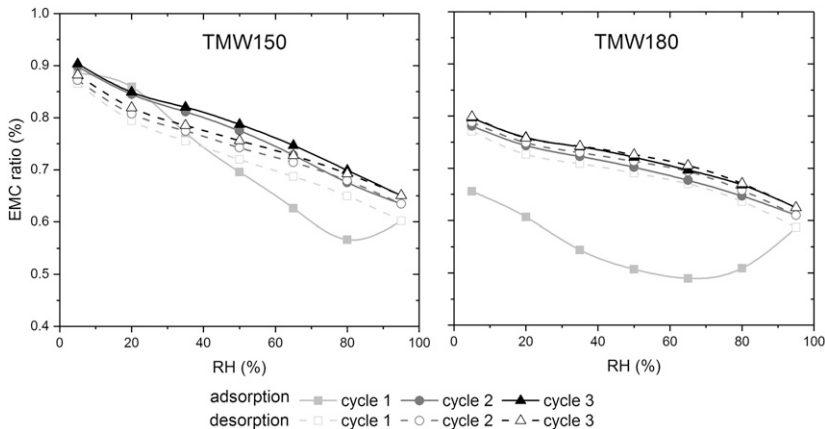


Figure 3.   EMC ratio of TMW150 and TMW180 related to unmodified wood (UW) calculated from the results in Figure 2, the solid lines with filled symbols represent the EMC ratio for adsorption. The dashed lines with open symbols represent EMC ratio for desorption. TMW, thermally modified wood.

higher value for the UW (1.75 $\pm$ 0.6 m$^2$/g) compared with TMW150 (1.6 $\pm$ 0.5 m$^2$/g) and TMW180 (1.3 $\pm$ 0.0 m$^2$/g). The results are in line with results from previous studies of unmodified and thermally modified spruce components (Källbom et al 2015) and unmodified spruce particles (Cordeiro et al 2012).

Figure 4 shows the dispersive surface energy heterogeneity for UW, TMW150, and TMW180. The results indicated an increase in the dispersive part of the surface energy as a result of thermal modification, implying a less hydrophilic character of the TMW samples. This is further supported by the chemical changes caused by the modification process, eg degradation of hemicellulose and softening and reorientation of the lignin giving the surface a more hydrophobic character (Sivonen et al 2002; Hill 2006). Higher thermal modification temperature (180°C) seemed to have more influence on the dispersive part of the surface energy than lower thermal modification temperature (150°C), comparing TMW180 and TMW150 in Figure 4. The highest value obtained at the lowest fractional surface coverage 1% ($n/n_\mathrm{m}^1 = 0.01$) was about 39.0 for UW mJ/m$^2$ and about 40.0 and 41.5 mJ/m$^2$ for TMW150 and TMW180, respectively. These results are in
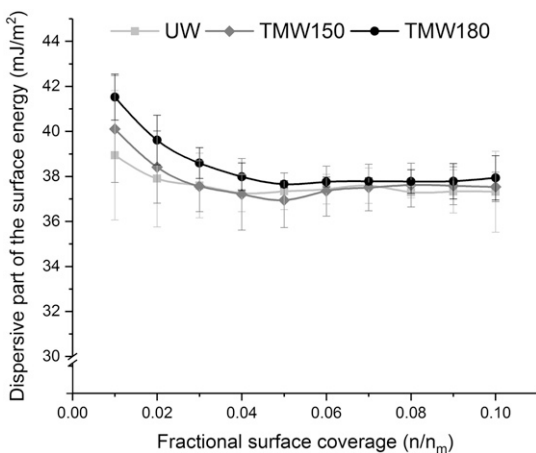


Figure 4.  Surface energy profiles showing the dispersive part ($\gamma^\mathrm{d}$) of the surface energy vs the fractional surface coverage for the unmodified (UW), and thermally modified (TMW) samples (TMW150 and TMW180). The results are based on three replicates per sample.

agreement with previous IGC studies on spruce components milled after thermal modification, with the maximum dispersive part of the surface energy about 44 mJ/m$^2$ for TMW and about 40 mJ/m$^2$ for UW samples (Källbom et al 2015). The larger difference between the UW and TMW samples in the latter study compared with this one is probably related to the higher modification temperature used (higher than 200°C). Another issue related to changes in surface properties is the migration of extractives to the surface (Kazaywoko et al 1997; Nuopponen et al 2003; Šernek et al 2004; Källbom et al 2015). Other studies of UW components from spruce showed similar results to this study; 42 mJ/m$^2$ (Wålinder and Gardner 2000; Peterlin et al 2010) and 41 mJ/m$^2$ (Cordeiro et al 2012). In previous studies of the surface energy of TMW from spruce determined by contact angle measurement, the dispersive part of the surface energy was increased, whereas the polar part was decreased with thermal modification temperature (Kutnar et al 2013; Altgen et al 2016a). Similar results were obtained for TMW pine (Gérardin et al 2007), and aspen (*Populus tremula*) and grey alder (*Alnus incana*) (Sansonetti et al 2013).

The acid-base properties are shown in Figure 5 as $K_\mathrm{A}$ and $K_\mathrm{B}$ numbers using the Gutmann approach, calculated from the specific free energy of adsorption of the polar probes. The $K_\mathrm{A}$ was lower than the $K_\mathrm{B}$ for all the samples; however, no clear difference was observed among the different samples in terms of acidity ($K_\mathrm{A}$). The $K_\mathrm{B}$, on the other hand, showed the highest values for TMW150, followed by TMW180 and UW samples. These results imply that mainly basic sites were involved in the adsorption process, ie surface functional groups with electron-donating properties. It is known that most wood species show a significantly higher base than acid number (de Meijer et al 2000). This is related to the basicity of lignin and the electron donor behavior of oxygen of its ether and carbonyl bonds (Mukhopadhyay and Schreiber 1995; Shen et al 1999; Riedl and Matuana 2006). About 35-70% of the linkages in the lignin biopolymer macromolecule are ether bonds (Klapiszewski et al 2017). The higher
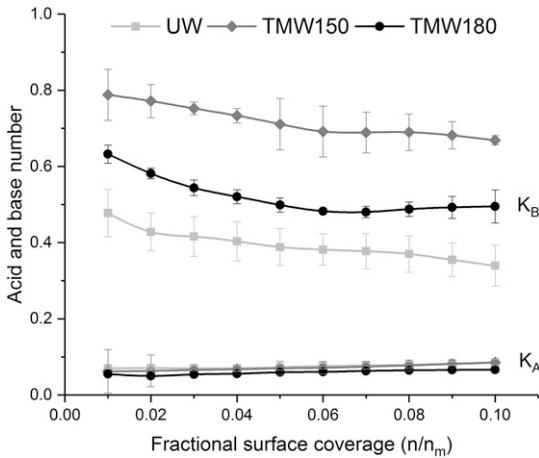
Figure 5.   The acid ($K_A$) and base ($K_B$) numbers vs the fractional surface coverage for the unmodified (UW), and thermally modified (TMW) samples (TMW150 and TMW180). The results are based on three replicates per sample.

dominant basicity of the TMW samples in this study could be related to the ether bonds in lignin and/or extractives (Tshabalala 1997), as a result of a relative increase of lignin and extractives at the surface caused by the thermal modification (Källbom et al 2016). At modification temperatures around 200°C (Fengel and Wegener 1984), these ether bonds will be cleaved. That might be the reason for lower $K_B$ numbers for TMW180 than for TMW150, where the latter one didn't reach temperatures high enough for ether bond-cleavage. Another reason could be related to depolymerization and repolymerization reactions, occurring at higher temperatures, leading to restructuring of lignin (Li et al 2007). With increasing temperature, lignin (Nuopponen et al 2004) and also extractives will be more easily extractable from the wood material. The acid-base numbers of UW are similar to those observed by earlier studies on UW from spruce: $K_A = 0.08$; $K_B = 0.33$ (Cordeiro et al 2012), and maple: $K_A = 0.15$; $K_B = 0.34$ (Wålinder and Gardner 2002).

## CONCLUSIONS

Water vapor sorption and surface energy properties of wood components (sawdust) are affected by thermal modification process conditions. As expected, the water vapor sorption properties were reduced for the TMW compared with UW samples with about 30-50% and a noticeable reversible reduction of the adsorption curve could further be seen for the first cycle compared with the subsequent cycles for the TMW samples. In addition, a smaller EMC ratio was observed for the adsorption of the TMW180 ($T = 180$°C, RH = 46%) compared with the TMW150 ($T = 150$°C, RH = 100%). The EMC ratio in the second and third sorption cycle decreased with increasing RH which could be caused by the formation of covalent bonds and repolymerization cross-linking reactions. The surface energy analysis indicated an increase of the dispersive part of the surface energy with increasing thermal modification temperature. The results from the acid-base properties showed a dominant basicity for all the samples with the highest base numbers ($K_B$) for TMW150, followed by TMW180 and UW. The higher $K_B$ for TMW was probably related to ether bonds from increased lignin and/or extractives content at the surface. The $K_B$ for TMW180 was lower than for TMW150, because of a higher thermal modification temperature of the first one, resulting in cleavage of the ether bonds. The results contribute to increased knowledge about water vapor sorption and surface properties of wood components after thermal modification. This information is useful for the understanding of the interaction between various wood components or prediction of their behavior in composite materials.

## REFERENCES

Altgen M, Militz H (2016) Influence of process conditions on hygroscopicity and mechanical properties of European beech thermally modified in a high-pressure reactor system. Holzforschung 70(10):971-979.

Altgen D, Avramidis G, Viöl W, Mai C (2016a) The effect of air plasma treatment at atmospheric pressure on thermally modified wood surfaces. Wood Sci Technol 50:1227-1241.

Altgen M, Hoffmann T, Militz H (2016b) Wood moisture content during the thermal modification process affects the improvement in hygroscopicity of Scots pine sapwood. Wood Sci Technol 50:1181-1195.

Altgen M, Willems W, Militz H (2016c) Wood degradation affected by process conditions during thermal modification of European beech in a high-pressure reactor system. Eur J Wood Wood Prod 74(5):653-662.

Andrade PI, de Oliveira Araújo S, Neiva DM, Vital BR, de Cássia Oliveira Carneiro C, Gominho J, Pereira H (2016) Strength properties and dimensional stability of particleboards with different proportions of thermally treated recycled pine particles. Holzforschung 70(5):467-474.

Borrega M, Kärenlampi PP (2008) Effect of relative humidity on thermal degradation of Norway spruce (Picea abies) wood. J Wood Sci 54:323-328.

Cordeiro N, Ornelas M, Ashori A, Sheshmani S, Norouzi H (2012) Investigation on the surface properties of chemically modified natural fibers using inverse gas chromatography. Carbohydr Polym 87:2367-2375.

de Meijer M, Haemers S, Cobben W, Militz H (2000) Surface energy determinations of wood: Comparison of methods and wood species. Langmuir 16:9352-9359.

Dorris GM, Gray DG (1980) Adsorption of n-alkanes at zero surface coverage on cellulose paper and wood fibers. J Colloid Interface Sci 77(2):353-362.

Endo K, Obataya E, Zeniya N, Matsuo M (2016) Effect of heating humidity on the physical properties of hydrothermally treated spruce wood. Wood Sci Technol 50(6):1161-1179.

Engelund ET, Klamer M, Venås TM (2010) Acquisition of sorption isotherms for modified woods by the use of dynamic vapour sorption instrumentation. Principles and practice. The International Research Group on Wood Protection, Doc. No. IRG/WP 10-40518.

Engelund ET, Thygesen LG, Burgert I (2017) Hydroxyl accessibility in wood cell walls as affected by drying and re-wetting. Cellulose 24(6):2375-2384.

Engelund ET, Thygesen LG, Svensson S, Hill CAS (2013) A critical discussion of wood-water interactions. Wood Sci Technol 47(1):141-161.

Esteves BM, Pereira HM (2009) Wood modification by heat treatment: A review. BioResources 4(1):370-404.

Fengel D, Wegener G (1984) Wood: Chemistry, ultrastructure, reactions. Walter de Gruyter & Co, Berlin. 613 pp.

Fowkes FM, Mostafa MA (1978) Acid-base interactions in polymer adsorption. Ind Eng Chem Prod Res Dev 17(1):3-7.

Gérardin P, Petrič M, Petrissans M, Lambert J, Ehrhardt JJ (2007) Evolution of wood surface free energy after heat treatment. Polym Degrad Stabil 92:653-657.

Gutmann V (1978) The donor-acceptor approach to molecular interactions. Springer US, New York. 279 pp.

Hill CAS (2006) Wood modification: Chemical, thermal and other processes. Wiley, Chichester. 260 pp.

Hill CAS, Norton AJ, Newman G (2010) The water vapour sorption properties of Sitka spruce determined using a dynamic vapour sorption apparatus. Wood Sci Technol 44: 497-514.

Hill CAS, Ramsay J, Keating B, Laine K, Rautkari L, Hughes M, Constant B (2012) The water vapour sorption properties of thermally modified and densified wood. J Mater Sci 47(7):3191-3197.

Himmel S, Mai C (2015) Effects of acetylation and formalization on the dynamic water vapor sorption behavior of wood. Holzforschung 69:633-643.

Hoffmeyer P, Jensen SK, Jones D, Klinke HB, Felby C (2003) Sorption properties of steam treated wood and plant fibres. Pages 177-189 in J van Acker and C Hill, eds. Proc. 11th European Conference on Wood Modification, April 3-4, 2003, Ghent, Belgium.

Källbom S, Sedighi Moghaddam M, Wålinder MEP (2018) Liquid sorption, swelling, and surface energy properties of unmodified and thermally modified Scots pine heartwood after extraction. Holzforschung 72:169-258.

Källbom S, Rautkari L, Wålinder M, Johansson L-S, Campbell JM, Segerholm K, Jones D, Laine K (2016) Water vapour sorption characteristics and surface chemical composition of thermally modified spruce (Picea abies karst.). Int Wood Prod J 7(3):116-123.

Källbom S, Wålinder MEP, Segerholm BK, Jones D (2015) Surface energy characterization of thermally modified spruce using inverse gas chromatography under cyclic humidity conditions. Wood Fiber Sci 47(4):410-420.

Kamdem DP, Bose SK, Luner P (1993) Inverse gas chromatography characterization of birch wood meal. Langmuir 9:3039-3044.

Kazaywoko M, Balatinecz JJ, Romansky M (1997) Thermodynamics of adsorption of n-alkanes on maleated wood fibers by inverse gas chromatography. J Colloid Interface Sci 190:408-415.

Klapiszewski Ł, Jamrozik A, Strzemiecka B, Matykiewicz D, Voelkel A, Jesionowski T (2017) Activation of magnesium lignosulfonate and kraft lignin: Influence on the properties of phenolic resin-based composites for potential applications in abrasive materials. Int J Mol Sci 18:1224.

Kutnar A, Kričej B, Pavlič M, Petrič M (2013) Influence of treatment temperature on wettability of Norway spruce thermally modified in vacuum. J Adhes Sci Technol 27(9): 963-972.

Legras A, Kondor A, Alcock M, Heiztmann MT, Truss RW (2017) Inverse gas chromatography for natural fibre characterization: Dispersive and acid-base distribution profiles of the surface energy. Cellulose 24:4691-4700.

Li J, Henriksson G, Gellerstedt G (2007) Lignin depolymerization/repolymerization and its crucial role for delignification of aspen wood by steam explosion. Biores Technol 98:3061-3068.

Lide DR, ed. (1995) CRC handbook of chemistry and physics, 76th edition. Pages 6-138, CRC Press, Boca Raton, FL.

Liu FP, Rials TG, Simonsen J (1998) Relationship of wood surface energy to surface composition. Langmuir 14:536-541.

Majka J, Czajkowski Ł, Olek W (2016) Effects of cyclic changes in relative humidity on the sorption hysteresis of thermally modified spruce wood. BioResources 11(2): 5265-5275.

Medved S, Humar M, Đalić M, Pohleve F (2012) Water and moisture resistance of particleboards made from thermally modified particles. Pages 353-358 *in* D Jones, H Militz, M Petrič, F Pohleven, M Humar, and M Pavlič, eds. Proc. 6th European Conference on Wood Modification, September 17-18, 2012, Ljubljana, Slovenia.

Militz H, Altgen M (2014) Processes and properties of thermally modified wood manufactured in Europe. Pages 269-285 *in* TP Schultz, B Goodell, and DD Nichols, eds. Deterioration and Protection of Sustainable Biomaterials, ACS Symposium Series. American Chemical Society, Washington, DC.

Mukhopadhyay P, Schreiber HP (1995) Aspect of acid-base interactions and use of inverse gas chromatography. Colloid Surf A Physicochem Eng Asp 100:47-71.

Nuopponen M, Vuorinen T, Jämsä S, Viitaniemi P (2003) The effects of a heat treatment on the behavior of extractives in softwood studied by FTIR spectroscopic methods. Wood Sci Technol 37:109-115.

Nuopponen M, Vuorinen T, Jämsä S, Viitaniemi P (2004) Thermal modifications in softwood studied by FT-IR and UV resonance Raman spectroscopies. J Wood Chem Technol 24(1):13-26.

Ormondroyd GA, Källbom SK, Curling SF, Stefanowski BK, Segerholm BK, Wålinder MEP, Jones D (2017) Water sorption, surface structure and surface energy characteristics of wood composite fibres refined at different pressures. Wood Mater Sci Eng 12(4):203-210.

Paul W, Ohlmeyer M, Leithodd H, Boonstra MJ, Pizzi A (2006) Optimising the properties of OSB by a one-step heat pre-treatment process. Holz Roh Werkst 64: 227-234.

Peterlin S, Planinšek O, Moutinho I, Ferreira P, Dolenc D (2010) Inverse gas chromatography analysis of spruce fibers with different lignin content. Cellulose 17:1095-1102.

Pfriem A, Zauer M, Wagenführ A (2010) Alteration of the unsteady sorption behavior of maple (*Acer pseudoplatanus* L.) and spruce (*Picea abies* (L.) Karst.) due to thermal modification. Holzforschung 64:235-241.

Riedl B, Matuana LM (2006) Inverse gas chromatography of fibers and polymers. Pages 3018-3031 *in* P Somasundaran, ed. Encyclopedia of Surface and Colloid Science, 2nd edition. Taylor & Francis, New York.

Runkel ROH (1954) Studien über die Sorption der Holzfaser. Erste Mitteilung: Die Sorption der Holzfaser in morphologische-chemischer Betrachtung. Holz Roh-Werkst 12:226-232 [in German].

Runkel ROH, Lüthgens M (1956) Untersuchungen über die Heterogenität der Wassersorption der chemischen und morphologischen Komponenten verholzter Zellwände. Holz Roh- Werkst 14:424-441 [in German].

Saint Flour C, Papirer E (1982) Gas-solid chromatography: A method of measuring surface free energy characteristics of short glass fibers. 2. Through retention volumes measured near zero surface coverage. Ind Eng Chem Prod Res Dev 21:666-669.

Sansonetti E, Andersons B, Biziks V, Grinins J, Chirkova J (2013) Investigation of surface properties of hydrothermally modified soft deciduous wood. Int Wood Prod J 4(2):122-127.

Schultz J, Lavielle L, Martin C (1987) The role of the interface in carbon fibre-epoxy composites. J Adhes 23(1):45-60.

Šernek M, Kamke FA, Glasser WG (2004) Comparative analysis of inactivated wood surface. Holzforschung 58: 22-31.

Shen W, Sheng YJ, Parker IH (1999) Comparison of the surface energetics data of eucalypt fibers and some polymers obtained by contact angle and inverse gas chromatography methods. J Adhes Sci Technol 13(8):887-901.

Sivonen H, Maunu SL, Sundholm F, Jämsä S, Viitaniemi P (2002) Magnetic resonance studies of thermally modified wood. Holzforschung 56:648-654.

Thielmann F, Burnett DJ, Heng JYY (2007) Determination of the surface energy distributions of different processed lactose. Drug Dev Ind Pharm 33:1240-1253.

Tjeerdsma BF, Boonstra M, Pizzi A, Tekeley P, Militz H (1998) Characterisation of thermally modified wood: Molecular reasons for wood performance improvement. Holz Roh- Werkst 56(3):149-153.

Tshabalala MA (1997) Determination of the acid-base characteristics of lignocellulosic surfaces by inverse gas chromatography. J Appl Polym Sci 65(5):1013-1020.

van Oss CJ, Good RJ, Chaudry MK (1988) Additive and nonadditive surface tension components and the interpretation of contact angles. Langmuir 4:884-891.

Weigl M, Schmidberger C, Müller U (2013) Water retention of wood particles—Characterization of polarity and particle size. Eur J Wood Wood Prod 71:147-151.

Wålinder MEP, Gardner D (2000) Surface energetics of extracted and non-extracted spruce wood particles studies by inverse gas chromatography (IGC). Wood Fiber Sci 32(4):478-488.

Wålinder MEP, Gardner D (2002) Acid-base characterization of wood and selected thermoplastics. J Adhes Sci Technol 16(12):1625-1649.

Willems W (2009) Novel economic large-scale production technology for high-quality thermally modified wood. Pages 31-35 *in* Proc. 4th European Conference on Wood Modification, April 27-29, 2009, Stockholm, Sweden.

Willems W, Altgen M, Militz H (2015) Comparison of EMC and durability of heat treated wood from high versus low water vapour pressure reactor systems. Int Wood Prod J 6:21-26.